Microb Ecol (2010) 60:561–571
DOI 10.1007/s00248-010-9662-1

HOST MICROBE INTERACTIONS

Effects of Sponge Bleaching on Ammonia-Oxidizing *Archaea*: Distribution and Relative Expression of Ammonia Monooxygenase Genes Associated with the Barrel Sponge *Xestospongia muta*

Susanna López-Legentil · Patrick M. Erwin · Joseph R. Pawlik · Bongkeun Song

Received: 6 November 2009 / Accepted: 22 March 2010 / Published online: 14 April 2010

Abstract Sponge-mediated nitrification is an important process in the nitrogen cycle, however, nothing is known about how nitrification and symbiotic *Archaea* may be affected by sponge disease and bleaching events. The giant barrel sponge *Xestospongia muta* is a prominent species on Caribbean reefs that contains cyanobacterial symbionts, the loss of which results in two types of bleaching: cyclic, a recoverable condition; and fatal, a condition associated with the disease-like sponge orange band (SOB) syndrome and sponge death. Terminal restriction fragment length polymorphism (TRFLP) analyses, clone libraries, and relative mRNA quantification of ammonia monooxygenase genes (*amoA*) were performed using a RNA transcript-based approach to characterize the active ammonia-oxidizing *Archaea* (AOA) community present in bleached, non-bleached, and SOB tissues of cyclically and fatally bleached sponges. We found that non-bleached and cyclically bleached tissues of *X. muta* harbored a unique *Crenarchaeota* community closely related to those reported for other sponges. In contrast, bleached tissue from the most degraded sponge contained a *Crenarchaeota* community that was more similar to those found in sediment and sand. Although there were no significant differences in *amoA* expression among the different tissues, *amoA* expression was higher in the most deteriorated tissues. Results suggest that a shift in the *Crenarchaeota* community precedes an increase in *amoA* gene expression in fatally bleached sponges, while cyclic bleaching did not alter the AOA community structure and its *amoA* gene expression.

S. López-Legentil (✉) · P. M. Erwin · J. R. Pawlik · B. Song
Center for Marine Science,
University of North Carolina Wilmington,
5600 Marvin K. Moss Lane,
Wilmington, NC 28409, USA
e-mail: susanna@univ-perp.fr

Present Address:
S. López-Legentil
Department of Animal Biology (Invertebrates),
University of Barcelona,
645 Diagonal Ave,
08028 Barcelona, Spain

Introduction

Nitrification is a fundamental process in the marine nitrogen cycle that makes fixed nitrogen available in the form of nitrite and nitrate to primary producers and for denitrification and anaerobic ammonium oxidation (anammox). Nitrification results from the combination of two processes: ammonia oxidation and nitrite oxidation. Ammonia oxidation is carried out by ammonia-oxidizing bacteria (AOB) belonging to the β and γ *Proteobacteria* [50], and by *Archaea* (AOA) from group I *Crenarchaeota* [25, 51, 64]. The relative importance of AOB and AOA in the nitrification process is still under investigation, although recent studies indicate that the nitrifying activity of AOA in marine ecosystems may equal or surpass the activity attributed so far to AOB [33, 70]. The ammonia oxidation process starts with the oxidation of ammonia to hydroxylamine, which is catalyzed by ammonia monoxygenase (AMO). The *amoA* gene encodes for the catalytic α-subunit of the AMO enzyme and has been widely used as a genetic marker to detect AOB [50]. The first putative archaeal *amoA* gene cluster was discovered from the sponge

symbiont *Cenarchaeum symbiousm* [25] and since then this gene has been suggested to be ubiquitous [14]. Recent advances in molecular techniques have made it possible to calculate *amoA* gene expression rates in environmental samples, revealing that marine *Crenarchaeota* are indeed capable of ammonia oxidation and could play a major role in ocean nitrification [6, 33].

Sponges are one of the most relevant groups in benthic marine ecosystems, a statement generally based upon their diversity and abundance [5, 7, 11, 22]. In addition to other well-established roles, including refugia for smaller invertebrates [11] and production of secondary metabolites with interesting pharmaceutical properties [47], most sponges also harbor an array of microorganisms, including cyanobacteria, aerobic and anaerobic microbes, and *Archaea* [4, 15, 26–29, 40, 41, 68, 69]. Some of these microorganisms also appear to play a critical role in the nitrogen cycle, notably in the nitrification process [3, 4, 12, 28, 30, 40, 52]. Several AOB and AOA have been detected in sponges by *amoA* and 16S rRNA gene sequencing, suggesting that these microorganisms actively metabolize nitrogen excreted by the sponge and its symbionts [3, 4, 13, 26, 28, 36, 39–41, 49, 55, 58, 59]. Hoffmann et al. [28] recently demonstrated that denitrification and anammox may also occur within sponge tissue through microbial processes, albeit at lower rates than nitrification.

Despite their predominance in many benthic marine communities, sponges are subject to direct and indirect anthropogenic disturbances and are endangered by disease outbreaks, and bleaching events [9, 20, 43, 65, 67]. The sponge *Xestospongia muta* (Demospongiae; Haplosclerida), also known as the giant barrel sponge, is one of the most common and largest inhabitants of Caribbean coral reef communities [1, 37, 38, 71]. Tissues of *X. muta* contain the sponge-specific, unicellular cyanobacterium *Synechococcus spongiarum* [23, 54, 63], in particular the sub-specific symbiont clades B and L [16]. Cyanobacterial symbionts in *X. muta*, and the closely related species *X. exigua* and *Neopetrosia subtriangularis*, appear to be commensals that provide no advantage to their sponge host [17, 35, 61]. Sponges have also been observed to totally or partially lose these cyanobacteria, a phenomenon known as sponge bleaching that has been reported to occur throughout the Caribbean [21, 42, 65]. Two types of bleaching have been reported for *X. muta*: cyclic and fatal bleaching [9, 35] (Fig. 1). Cyclic bleaching results in a spotty appearance to the sponge, as the affected tissue loses its reddish-brown coloration and becomes off-white, and occurs in ~25% of the sponge population off Key Largo, Florida [9]. Cyclic bleaching does not appear to stress the sponge, and affected individuals recover over time [35]. Fatal bleaching, on the other hand, affects less than 1% of Florida barrel sponges and resembles an infection that results in partial or total tissue loss and sponge death [9]. Fatal bleached sponges have three distinct tissue types: (1) a healthy reddish-brown tissue (hereafter called normal); (2) a totally bleached and dying tissue (hereafter called bleached); and (3) a bright orange band that migrates across the sponge and separates the normal and the bleached tissues (hereafter called SOB). Although reports of sponge disease and bleaching are increasing worldwide [67], to date, no study has attempted to determine the effect of these phenomena on the symbiotic ammonia-oxidizing community within sponge tissues.

The main goals of this study were to describe and compare the archaeal diversity present in Caribbean giant barrel sponges undergoing cyclic and fatal bleaching, and to determine the relative expression of the *amoA* gene in the different tissues (normal, bleached, and SOB). To achieve these objectives, we first compared the archaeal communities present in the normal and bleached tissue of three cyclic beaching sponges, and the normal, bleached and SOB tissue of three fatally bleached sponges by terminal restriction fragment length polymorphism (TRFLP) analysis of the *amoA* gene transcripts. We then constructed clone libraries of the *amoA* gene to determine the identity of the major TRFLP peaks and established their phylogenetic relationship with *amoA* genes from other invertebrate hosts and environmental samples. Finally, we assessed the relative mRNA abundance of the *amoA* gene in these same tissues using quantitative real-time PCR (QRT-PCR).

Materials and Methods

Sample Collection

Samples from the giant barrel sponge *X. muta* were collected from Conch Reef (24°57′13″N; 80°27′13″W) and Conch Wall (24°57′01″N; 80°27′25″W), Key Largo, Florida. Sponges undergoing fatal bleaching belonged to one of the following two categories: (1) early stage of fatal bleaching, meaning that the sponge still has its typical barrel shape and more than 50% of living tissue (samples B10 and B11; Fig. 1a), and (2) late stage or advanced fatal bleaching, where there was less than 10% living tissue remaining and the sponge had started disintegrating, thereby losing its barrel shape (sample B9; Fig. 1b). From each fatally bleached sponge, samples of bleached tissue, sponge orange band (SOB) tissue, and normal colored tissue (non-bleached) were collected in individual sealed plastic bags. Once on board of the ship, tissue cores were taken from each sponge using a 7-mm diameter cork borer and immediately dropped in liquid nitrogen until transferred to a −70°C freezer. For each cyclic bleached sponge (B12, B13, B14; Fig. 1c), two sub-samples per individual were

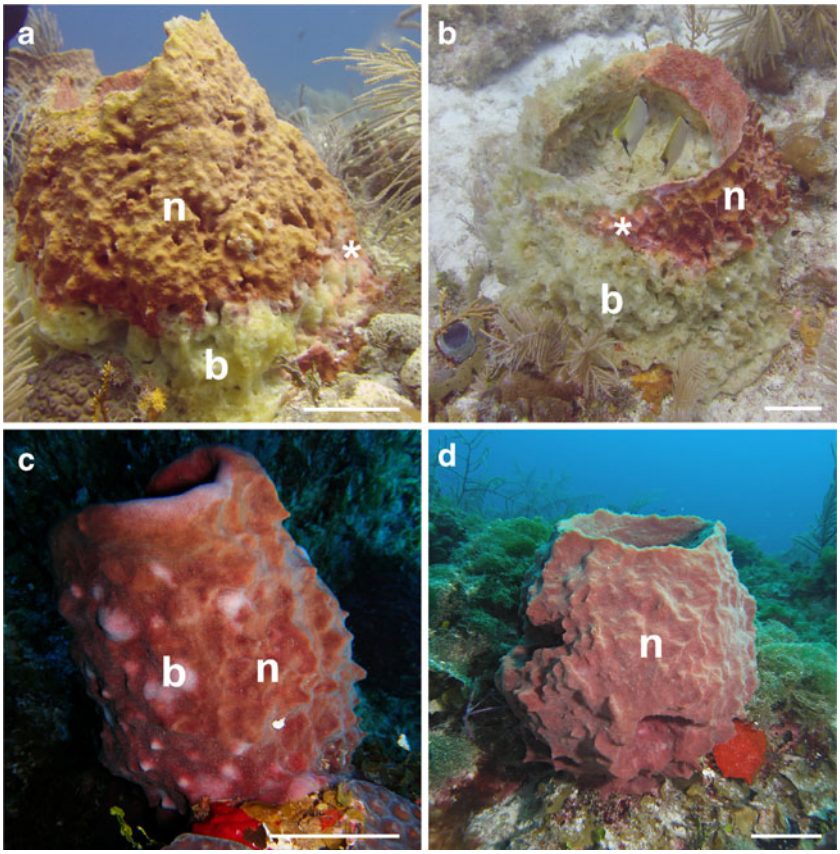

Figure 1 The giant barrel sponge *X. muta* in Conch Reef and Conch Wall, Florida. **a** Early stage of fatal bleaching; **b** late stage of fatal bleaching; **c** cyclic bleached sponge; and **d** unbleached sponge. *Asterisks* indicate the orange band of fatal bleached sponges (SOB), *n* unbleached tissue, and, *b* bleached tissue. *Scale bar*=10 cm

collected: bleached and normal tissue. Tissue types were classified by visual inspection and areas bordering other tissue types were avoided. Samples were collected by SCUBA diving in June 2006.

Restriction Enzyme Digestion and TRFLP Analysis from *AmoA* Transcripts

RNA was extracted from sponge samples as described by López-Legentil et al. [35]. The utilization of RNA instead of DNA ensured that amplifications were obtained only from living microorganisms. Reverse transcription and amplification was performed using RNA samples, the primer set [6'FAM]Arch-amoAF and Arch-amoAR, and the SuperScript™ One-step RT-PCR for long-templates (Invitrogen, Carlsbad, CA, USA). Samples were run in a 1% agarose gel and bands of ~650 bp were purified using the Wizard® SV gel and PCR cleanup system (Promega, Madison, WI, USA). The concentration of the purified cDNA was measured using the Quant-iT Qubit® kit (Invitrogen). Approximately 20 to 50 ng of purified PCR products were digested with 0.5 μl of the restriction endonucleases *HaeIII* (Promega), 2 μl Buffer C, 0.2 μl BSA, and nuclease-free water to a total volume of 10 μL. All digests were incubated at 37°C overnight. Immediately following digestion, samples were precipitated with 75% isopropanol and resuspended with 10 μl Hi-Di formamide and 0.5 μl of GeneScan 500 ROX (Applied Biosystems, Foster City, CA). Fragments were loaded on an automated sequencer ABI Prism 3100 and analyzed using GeneMapper v 4.0 (Applied Biosystems). Only fragment lengths in the range of 60 to 600 nucleotides were considered for further analysis. Raw TRFLP peak profiles were standardized using a proportional threshold of total fluorescence [44] and compared across samples using T-REX (alignment threshold=1.5 bp) [10]. Individual TRFs with peak areas less than 0.5% relative fluorescence were discarded as background noise. Proportional fluorescence calculations yield a measure of the relative abundance of TRF peaks and the gene sequences they represent, with larger peak sizes correlating to higher numbers of amplicons in PCR product mixes.

To match recovered clone sequences to TRF peaks in TRFLP profiles, in silico digestions were performed in BioEdit version 7.0.5.2 [24]. Cut sites at the 5′-end of each sequence were identified based on the recognition sequence

of the restriction endonuclease *HaeIII* (GG'CC) and utilized to predict the corresponding length of sequences in TRFLP profiles to match predicted TRFs to empirically derived TRFs. Extrapolations from clone libraries to TRFLP profiles were used to empirically validate the specificity of individual TRFs. Although the presence of additional *amoA* gene sequences that match specific TRFs but are not represented in clone libraries cannot be excluded, the likelihood of such an occurrence decreases as the number of sequenced clones increases.

AmoA Clone Library Construction

Bleached, normal, and orange band tissue from *X. muta* sample B9, and bleached tissue from sample B11 were collected, RNA extracted, and reverse-transcribed as indicated above. The primer set Arch-amoAF and Arch-amoAR described in Francis et al. [19] was used to amplify a fragment of the *amoA* gene. Total reaction volume was 25 μL with: 12.5 μL of 2× reaction mix, 0.5 μL of each primer (10 μM), 0.5 μL RT/Platinum Taq polymerase, 10 μL of PCR grade water and 1 μL RNA. A first incubation of 30 min at 50°C was followed by a single soak at 94°C for 2 min, 35 amplification cycles (denaturation at 94°C for 15 s; annealing at 53°C for 30 s; and extension at 68°C for 1 min), and a final extension at 72°C for 5 min, in a Peltier PTC-200 gradient PCR. The normal tissue from sample B14 was DNA extracted using the Puregene kit (Gentra Systems, Minneapolis, MN, USA). The same primer set and amplification reaction mentioned above was used, except for the first incubation step at 50°C which was not performed. RT-PCR and PCR products were run in a low-melting-point agarose gel (1%), purified using PerfectPrep Gel Cleanup (Eppendorf, Hamburg, Germany), and cloned in *Escherichia coli* using the TOPO® TA Cloning® Kit and One Shot® TOP10 competent cells, according to manufacturer's instructions (Invitrogen). White clones were hand-picked, transferred to a 96-well culture plate containing 125 μL of LB liquid media and kanamycin, and allowed to grow overnight at 37°C. Clone libraries were screened by PCR using the plasmid primers T7 and M13R and a total reaction volume of 25 μL:1 μL of each primer (10 μM), 0.5 μL dNTP's (10 mM), 2.5 μL 10× buffer, 2 μL $MgCl_2$, 0.5 μL Taq polymerase 5U, 16.5 μL of PCR grade water, and 1 μL of each clone, and the following cycle parameters: a single soak at 95°C for 10 min, followed by 30 amplification cycles (95°C for 30 s; 55°C for 30 s and 72°C for 1.5 min), and a final step at 72°C for 2 min. PCR amplicons were run in a low-melting-point agarose gel (1%) to confirm insert size previous to sequencing using BigDye TM terminator v. 3.1 and the same primers used in the amplification step on an ABI Prism 3100 automated sequencer.

Phylogenetic Analysis of *AmoA* Sequences

To perform phylogenetic analyses, partial *amoA* sequences were retrieved from GenBank (Fig. 2). Relationships between *amoA* sequences were established with the neighbor-joining (NJ) algorithm, and maximum parsimony (MP) analyses using Mega v 4 [56]. For NJ analysis, the Kimura 2-Parameter model of nucleotide substitution was used and data were re-sampled using 10,000 bootstrap replicates [18]. For MP analysis, a heuristic search was performed with ten random addition replicates, and confidence in the nodes was assessed by 5,000 bootstrap replicates. Modeltest v 3.8 [48] was used to select the best-fit model of DNA substitution for maximum likelihood (ML) analysis. Comparisons between the different likelihood scores showed that the GTR+I+G model (General time reversible) [57] was the best-fit model for nucleotide substitution. Using Treefinder v October 2008 [31] and 10,000 bootstrap replicates, a tree was constructed under the maximum likelihood criterion and the GTR+I+G parameters. All sequences have been deposited in the GenBank data base (Acc. nos. GQ485687 to GQ485795).

QRT-PCR Primer Design

For *amoA* gene, sequences obtained from the clone library were aligned with other *amoA* gene sequences retrieved from GenBank using Bioedit version 7.0.5.2 [24] and ClustalX [62]. A consensus sequence was then created to design the QRT-PCR primer set ARAMORT1F 5′-GCATCAGTGTCTGCGATATTG-3′ (forward) and ARAMORT1R 5′-TGGCTTAGACGATGTACCCAC-3′ (reverse) targeting a 101-bp region of the detected *amoA* gene. To design QRT-PCR primers for 16S rRNA, DNA of frozen tissue from four different sponges was extracted using the Puregene kit (Gentra Systems). Archaeal sequences for the 16S rRNA gene were obtained using the primer set Parch 519f [45] and ARC915r [53]. 16S rRNA fragments were amplified after running a PCR with a single soak at 95°C for 5 min, followed by 35 amplification cycles (denaturation at 95°C for 15 s; annealing at 55°C for 15 s; and extension at 68°C for 1 min), and a final extension at 72°C for 5 min in a Peltier PTC-200 gradient PCR (MJ Research). Amplification products were purified by cutting out the appropriate band from a low-melting-point agarose gel (1%) and using PerfectPrep Gel Cleanup (Eppendorf). The purified DNA was cloned in *E. coli* using the TOPO® TA Cloning® Kit and One Shot® TOP10 competent cells, according to manufacturer's instructions (Invitrogen). Thirteen positive colonies were sequenced using BigDye TM terminator v. 3.1 and the same primers as in the amplification step. Sequences were obtained on an ABI Prism 3100 automated sequencer. Sequences have

been deposited in the GenBank (GenBank acc. nos. GQ485796 to GQ485806). Other sequences corresponding to 16S rRNA from *Crenarchaeota* were retrieved from GenBank and aligned with ours to create a consensus sequence and design the QRT-PCR primers Arch16SF 5′-GGGAGTGGGAGAGGTAGAC-3′ (forward) and Arch16SR 5′-GTCGGACGTGTTCTGGTAG-3′ (reverse) targeting a 101-bp region. All primers for QRT-PCR were designed using the Primer Express software (Applied Biosystems).

RNA Extraction, cDNA Synthesis, and QRT-PCR Analyses

Approximately 90 mg of frozen tissue at −70°C was homogenized in TRIzol® reagent (Invitrogen) and then processed using the Micro-to-Midi RNA purification kit (Invitrogen) to obtain purified RNA in 100 μL nuclease-free water. All samples were DNAse treated with DNase Amplification Grade I (Invitrogen) according to manufacturer's instructions. For cDNA synthesis, ~400 ng of total RNA was reverse-transcribed using SuperScript Reverse Transcriptase II kit (Invitrogen) with specific primers targeting either *amoA* gene or 16S rRNA gene. To quantify mRNA abundance of the *amoA* gene, the standard curve method was used in a 7500 Applied Biosystems quantitative real-time PCR. Standards for 16S rRNA gene (reference gene) and *amoA* gene (target gene) were obtained by cloning (TOPO TA Cloning® Kit, Invitrogen). Positive colonies were analyzed by PCR using the plasmid primers T7 and M13R and the same PCR reaction mentioned in the 'clone library construction' section. Colonies containing the correct insert were grown overnight in liquid LB medium (10 g tryptone, 5 g yeast extract, and 10 g agar in 1 L of distilled water) supplemented with 50 μg/ml of kanamycin. Plasmid extraction was performed using the Perfectprep plasmid Mini kit (Eppendorf) and sequenced to re-verify that the correct fragment of 16S rRNA or *amoA* gene was present. QRT- PCR reactions were performed with 3 μL of *amoA* or 16S rRNA cDNA in 10 μL SYBR greener supermix (Invitrogen), and nuclease-free water to a total volume of 20 μL. The QRT-PCR was run with the following cycle parameters: a single soak at 50°C for 5 min and 95°C for 10 min, was followed by 40 amplification cycles (95°C for 15 s; 50°C for 15 s; and 68°C for 0.35 s). Each 96-well plate contained two negative controls, samples in triplicates, and sevenfold serial dilutions of the corresponding standard. Samples from a same treatment set were analyzed together. Melt curve analysis and agarose gel electrophoreses were performed following each PCR to check for the specificity of the PCR products. Fold change in the target gene and the reference gene were calculated as indicated by López-Legentil et al. [35].

Data Analysis

In order to standardize *amoA* expression data for bleached sponges, samples of normal tissue (non-bleached) were considered controls. For fatally bleached sponges, bleached and orange band tissues were considered experimental samples. For cyclically bleached sponges, bleached tissue was considered the experimental sample. Differences between normal tissue and bleached and orange band tissues were assessed using a paired *t* test, and differences among ratios of *amoA* expression using an ANOVA on ranks. The statistical package SigmaPlot v 11 was used for all the analyses.

Results

Restriction Enzyme Digestion and TRFLP Analysis of *AmoA* Gene Transcripts

TRFLP analysis with the restriction endonuclease *HaeIII* yielded a total of 12 unique TRFs (Table 1). Three dominant TRFs (TRF-1, -2, -3) were detected from all sponge tissue types (normal, bleached and diseased) and appeared in >50% of TRFLP profiles (Table 1). TRF-1 appeared in all TRFLP profiles and dominated most archaeal communities, averaging 68% relative fluorescence (Table 1). TRF-4 was detected solely from fatally bleached sponge tissue and dominated the archaeal community of the fatally bleached sponge B9, which was in the latest stage of degradation (97.3% relative fluorescence, Table 1). Notably, the dominance of TRF-4 in sponge B9 was at the exclusion of TRF-1, reduced to 2.7% relative abundance. TRF-4 was also detected in low abundance in the fatally bleached sponge B10 (early stage; 2.7% relative fluorescence). Thus, while TRF-1, TRF-2, and TRF-3 appeared in all tissues of cyclically and fatally bleached sponges, TRF-4 only appeared in the bleached tissue of fatally bleached sponges. The additional eight TRFs were found in low relative abundance and were not represented by *amoA* sequences from the clone library analyses. TRF-7 was isolated from fatally bleached tissue in the sponge B11, while TRF-9 was found in both normal and fatally bleached tissue at very low (<1% relative fluorescence) abundances (Table 1). The remaining 6 TRFs (TRF-5, -6, -8, -10, -11, -12) were recovered solely from sponge orange band tissue and found in low abundance (<6% relative fluorescence, Table 1).

Phylogenetic Analysis of *AmoA* Sequences

A total of 109 partial *amoA* gene sequences (636 bp) were recovered from the giant barrel sponge *X. muta*; including

Support Values

Clade	NJ	MP	ML
①	82	-	91
②	98	87	99
③	90	-	81
④	99	79	-
⑤	82	-	-
⑥	100	99	99
⑦	87	-	69
⑧	99	99	99
⑨	98	83	87
⑩	100	99	100
⑪	100	99	100
⑫	100	99	100
⑬	100	99	99
⑭	99	97	100
⑮	100	99	100
⑯	91	62	70
⑰	99	-	53
⑱	80	-	-
⑲	76	-	94
⑳	50	-	-
㉑	94	94	99
㉒	-	-	67
㉓	87	50	55
㉔	100	99	99
㉕	52	54	96
㉖	-	-	83
㉗	70	-	77
㉘	60	-	-
㉙	90	-	65
㉚	99	95	99
㉛	99	99	99
㉜	70	55	-
㉝	100	99	100
㉞	54	-	-
㉟	54	-	-
㊱	71	74	89
㊲	82	-	62
㊳	59	51	55
㊴	100	99	100
㊵	100	99	96
㊶	83	-	-
㊷	100	99	100
㊸	99	99	100
㊹	96	78	97
㊺	100	99	100

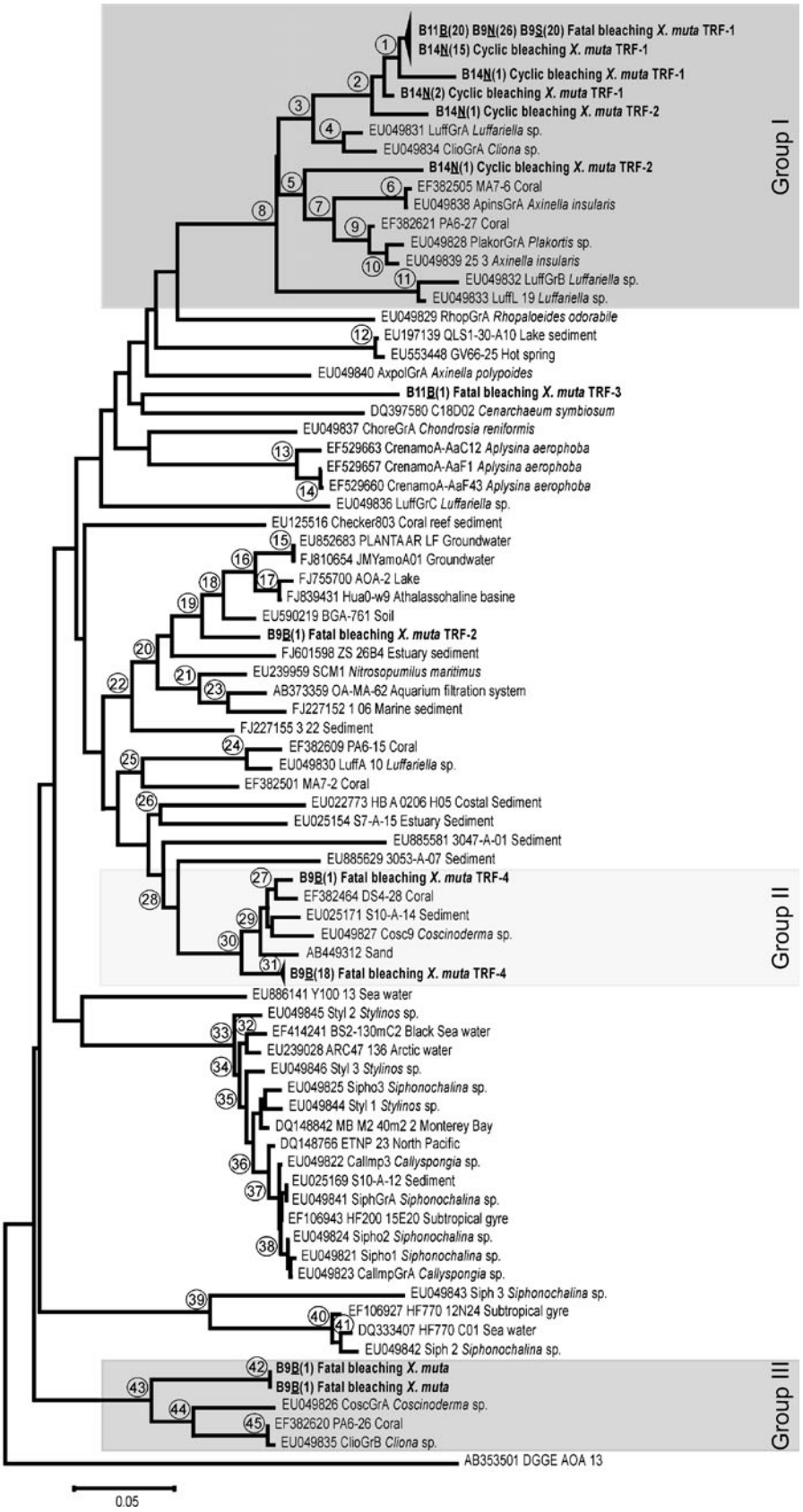

Figure 2 Phylogeny of partial *amoA* gene sequences from uncultivated *Crenarchaeota* from the tissue of the giant barrel sponge *X. muta* (*in bold*), and retrieved from NCBI GenBank. Labels on terminal nodes of reference sequences indicate GenBank accession numbers, clone name, and sample source (species name for sponge-derived sequences). Labels on terminal nodes of sequences from this study include sample name (*B9*, *B11*, or *B14*), tissue analyzed (*underlined B* bleached, *S* orange band, *N* normal), number of sequences (*in parenthesis*), bleached status (cyclic vs. fatal), and TRF match. *Dark gray bars* highlight clades exclusively formed by symbiotic (sponge- and coral-associated) *Crenarchaeota* sequences. The light gray bar signals a mixture of clades formed by both free-living and host-related *Crenarchaeota*. Tree topology was obtained from neighbor-joining (NJ) analysis. Individual bootstrap values from NJ, MP and ML analyses are located in the upper-left corner and correspond to circle numbers on tree nodes. *Scale bar* represents 0.05 substitutions per site

20 from normal tissue, 20 from SOB tissue, and 69 from fatally bleached tissue. All sequences obtained corresponded to marine group I *Crenarchaeota*. Phylogenetic analysis revealed three well-supported clades including most of the sequences obtained in this study (Fig. 2). The first group (Group I; Fig. 2 dark gray bar) formed a monophyletic clade exclusively comprised of *amoA* sequences isolated from a host organism (i.e., sponges or corals) supported by bootstrap values >99%. All sequences obtained from normal tissue of fatal and cyclic bleaching sponges and SOB tissue were found in this group. According to in silico digestions, TRF-1 matched to a tight phylogenetic cluster within this group formed by 84 sequences averaging 1.0% sequence divergence (Table 2, Fig. 2). Two out of the three sequences matching TRF-2 were also present in group I, while the third sequence grouped in a well-supported clade with sequences retrieved from water, sediment and soil samples (Fig. 2).

The second well-supported group of sequences (Group II; Fig. 2 light gray bar) was formed by both free-living and host-related *Crenarchaeota* and included sequences obtained from marine sediment, sand, corals and sponges. This group also contained most of the sequences obtained from the bleached tissue of sample B9 (late stage of fatal bleaching; see experimental procedures) and matched TRF-4 (average sequence divergence 1.22%; Table 2). The third group (Group III, Fig. 2 dark gray bar) was supported by bootstrap values >99%, contained two *amoA* sequences from fatally bleached tissue (B9) and also formed a monophyletic clade with symbiotic (sponge- and coral-associated) *Crenarchaeota* sequences. Group III was not represented in recovered TRFLP profiles. In silico digestions of group III sequences revealed a *HaeIII* recognition site at 632 bp, outside the accurate range of TRFLP analyses and the range considered herein (60 to 600 bp, see experimental procedures). Finally, a single sequence from the bleached tissue of sample B11 (early stages of fatal bleaching) matched TRF-3 (Table 2), and appeared amid other sponge-related sequences. However, this sequence did not form a bootstrap supported clade with any other sequence. Thus, three main groups were retrieved through phylogenetic analysis of *amoA* sequences: Group I and III were exclusively formed by symbiotic (sponge- and coral-associated) *Crenarchaeota* sequences, while group II contained a mixture of clades formed by both free-living and host-related *Crenarchaeota*.

QRT-PCR Analyses of *AmoA* Gene Transcripts

There were no significant differences in *amoA* gene expression between bleached and normal tissue from

Table 1 Summary results of TRFLP analysis highlighting the size, presence (number and percentage of total profiles), abundance (relative fluorescence), sample name and tissue analyzed (italicized, B = bleached, S = orange band, N = normal), and tissue specificity of each recovered TRF

Fragment	Empirical size (bp)	No. TRFLP profiles	Fluorescence (Rel., Avg±SE)	Samples	Tissue specificity
TRF-1	249.65	15 (100%)	68.0±5.8%	All	All
TRF-2	347.29	14 (93%)	17.6±3.2%	All except B9*B*	All
TRF-3	474.96	9 (60%)	12.2±3.5%	B9*N*, B10*B*, B10*S*, B10*N*, B11*N*, B12*B*, B12*N*, B13*B*, B13*N*	All
TRF-4	109.75	2 (13%)	50.0±47.3%	B9*B*, B10*B*	Fatal bleach
TRF-5	477.3	1 (7%)	5.30%	B11*S*	SOB
TRF-6	568.25	1 (7%)	4.40%	B9*S*	SOB
TRF-7	549.13	1 (7%)	4.20%	B11*B*	Fatal bleach
TRF-8	82.78	1 (7%)	3.10%	B9*S*	SOB
TRF-9	207.23	3 (20%)	0.7±0.1%	B9*S*, B11*S*, B14*N*	Normal, SOB
TRF-10	234.02	1 (7%)	1.10%	B9*S*	SOB
TRF-11	111.63	1 (7%)	0.92%	B9*S*	SOB
TRF-12	344.56	1 (7%)	0.52%	B9*S*	SOB

Rel. relative, *SOB* sponge orange band, *Fatal bleach* fatally bleached tissue

Table 2 Clone library *amoA* sequence matches to dominant TRFs from TRFLP analysis

Fragment	Empirical size (bp)	Predicted size (bp)	No. Clone matches	No. Unique sequences	Divergence (Avg ± SE)	Divergence range	Clade specific
TRF-1	249.65	250	84	38	1.0±1.1%	0.2–6.3%	Group I
TRF-2	347.29	347	3	3	16.5±6.6%	9.0–21.2%	No
TRF-3	474.96	478	1	1	–	–	No
TRF-4	109.75	112	19	15	1.2±1.4%	0.2–6.0%	Group II

Predicted size indicates the in silico digestions of *amoA* transcripts with the restriction enzyme *HaeIII*, and divergence denotes pairwise nucleotide distances among sequence clusters. Clade specific refers to monophyletic archaeal sequence groups in Fig. 2

sponges undergoing cyclic bleaching (p=0.415) and fatal bleaching (p=0.225), or between SOB and normal tissue of fatally bleached sponges (p=0.782; Fig. 3). No significant differences were detected either among ratios of *amoA* expression in bleached tissues of cyclic and fatal bleaching sponges, and SOB tissue (p=0.339). The large standard deviation bar observed for the bleached tissue of fatally bleached sponges depicted in Fig. 3 (±44.94; SE) was largely due to sample B9 (late stage of fatal bleaching), which presented a relative level of *amoA* expression higher than fatal bleaching sponges in an earlier degradation stage (136.95 vs. 1.15 and 3.11, respectively). Accordingly, sample B9 also presented higher levels of *amoA* expression in SOB tissue (23.11 vs. 0.69 and 0.29 for samples in early stage of fatal bleaching). No such intra-specific variation was observed for sponges undergoing cyclic bleaching, with all sponges having an average ratio of *amoA* gene expression in their bleached tissue of 0.86 (±0.211; SE).

Discussion

Studies of archaeal communities in sponges have provided ample evidence of specific sponge- *Crenarchaeota* associations [29, 34, 36, 46, 55, 68, 69]. In this study, we described a new sponge-specific archaeal association for the giant barrel sponge *X. muta* (Fig. 2, groups I and III). The *Crenarchaeota* sequences in groups I (matching TRF-1) and III were retrieved from both cyclically and fatally bleached sponges and were similar but not identical to the ones described for other demosponge species (i.e., *Cliona*; *Luffariella*; *Axinella*; *Plakortis*; and *Coscinoderma*). Except for one, all sequences retrieved from the bleached tissue of the most degraded sponge (B9) matched TRF-4 and were highly similar to free-living *Crenarchaeota* (e.g., sand- and sediment-derived sequences), and a few other sequences obtained from sponge or coral hosts (Fig. 2, group II). Corals rely on the photosynthetic products of zooxanthellae for the majority of their nutrients,

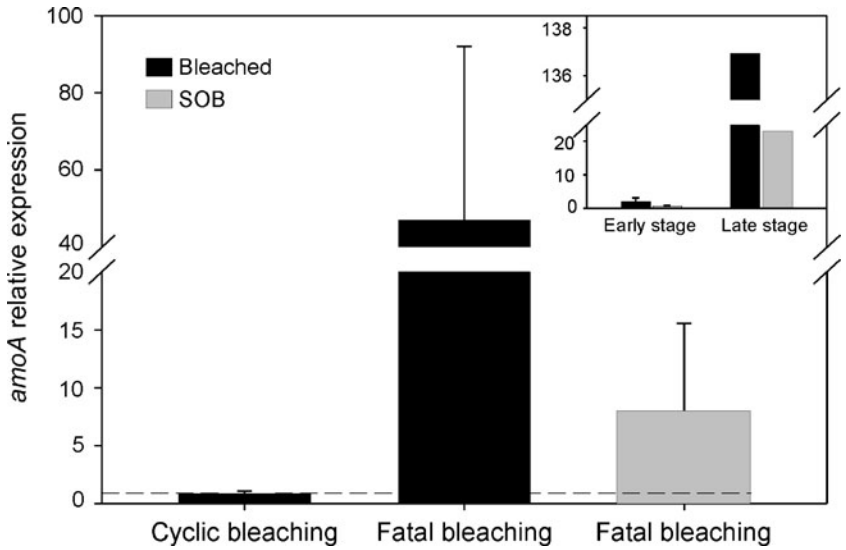

Figure 3 Relative levels of *amoA* gene expression in sponges undergoing cyclic and fatal bleaching in Conch Reef, Florida. *AmoA* levels were determined as a ratio between bleached tissue or tissue from the sponge orange band (SOB) and normal tissue (non-bleached). *Dotted lines* indicate a ratio of one. *Inset* represents *amoA* expression in early and late stages of fatal bleaching (*Y* axis units same as main panel). *Bars* indicate standard error

but also capture zooplankton with their polyps and collect fine particles in mucous films. Sponges obtain their nutrition by filtering the surrounding water column and by subsequent phagocytosis of the captured particles, included microorganisms. In addition, some sponges are also known to incorporate and store sediment particles in their tissues [2, 8, 60]. Therefore, it is expected that some *Crenarchaeota* sequences obtained from sponges and corals would present higher similarities with free-living phylotypes, such as those from group II (Fig. 2), than with specific sponge symbionts.

Cyclic bleaching did not alter the existing *Crenarchaeota* community in the sponge. Both normal and bleached tissue of cyclically bleached sponges presented equivalent TRFLP profiles and *amoA* sequences (Table 1, Fig. 2). No significant changes in relative *amoA* gene expression were detected either (Fig. 3). These results are in accordance with a previous study suggesting that this type of bleaching is due to a temporary decrease in cyanobacterial density and has no effect on sponge physiology [35]. In contrast, we found that in the earlier stages of fatal bleaching the relative expression of *amoA* gene appeared to decrease in SOB tissues but slightly increased in bleached tissues (samples B10 and B11; Fig. 3). As tissue bleached and died, the unique sponge-associated *Crenarchaeota* forming the phylogenetic group I (TRF-1 and TRF-2) was altered by the appearance of new *Crenarchaeota* sequences, which were detected in both TRFLP profiles and clone libraries (Table 1, Fig. 2). The presence of new TRFs exclusively associated with SOB tissue (TRF-5, TRF-6, TRF-8, and TRF-10 to 12; Table 1) may signal the disruption of the natural *Crenarchaeota* community due to disease progression. Finally, a completely new community characterized by a group of sequences resembling free-living *Crenarchaeota* (TRF-4 in Table 1 and Group II in Fig. 2), occupied the bleached tissue of the most degraded sponge (B9), and started to appear in the bleached tissue of sponge B10 (early stage of fatal bleaching; Table 2).

The appearance of a new *Crenarchaeota* community in the highly degraded tissue of sponge B9 was detected by TRFLP and *amoA* sequence analyses and corresponded to higher *amoA* gene expression (Figs. 2 and 3, Table 1). The relative increase in gene expression could be due to greater release of ammonia from tissue degradation [66], or to the shift in the *Crenarchaeota* community itself. Since QRT-PCR assays were normalized using specific primers designed for *Crenarchaeota* 16S rRNA, the relative increase in *amoA* gene expression could also be due to a higher number of *amoA* copies per cell in the *Crenarchaeota* community that characterized the bleached tissue of sample B9. In fact, evidence to date suggests that crenarchaeotal cells may possess 1 to 3 copies of *amoA*, depending on the phylotype [70]. However, as sponge B9 also had higher *amoA* gene expression in its SOB tissue than sponges B10 and B11 but presented the same *Crenarchaeota* community than the later, our results seem to support the hypothesis that ammonia released by tissue death is the main reason for higher expression of *amoA* genes in highly degraded sponges. A shift in microbial functional potential has also been reported between healthy and diseased coral. Specifically, the number of nitrification genes in the surface mucopolysaccharide layer of yellow band diseased *Montastrea faveolata* was 60% higher than that associated with healthy corals [32].

In conclusion, we found that tissues from the giant barrel sponge *X. muta* were associated with a specific group of *Crenarchaeota*. Cyclic bleaching did not alter the community structure of these symbionts nor their *amoA* gene expression, while the progressive loss of sponge tissue from fatal bleaching yielded a disruption of the sponge-specific *Crenarchaeota* community. A *Crenarchaeota* community that was more similar to those found in sediment and sand appeared to replace the sponge symbionts in the more degraded tissues, followed by a relative increase of *amoA* gene expression probably due to the higher release of ammonia after tissue death (Fig. 3). The presence of unique *Crenarchaeota* communities within *X. muta* tissues (group I and III in Fig. 2, and TRF-1 in Table 1) and their gradual loss and substitution by free-living *Archaea* following tissue death (group II in Fig. 2, and TRF-4 in Table 1) suggest an obligate symbiosis between host and microorganism. The strength and type of association (e.g., commensalism, parasitism) between sponges and *Archaea* remains undetermined but results point toward a parallel evolution and some degree of involvement in sponge metabolism [29, 39]. This study shows that neither the community structure of *Crenarchaeota* symbionts nor their *amoA* gene expression appear to be affected by sponge bleaching, unless this process is accompanied by tissue death and sponge morbidity.

Acknowledgments Steve McMurray and Dr. Timothy P. Henkel helped with sponge sampling. Tenesha J. Vereen helped with sequencing. This study was supported by grants from NOAA's Undersea Research Center at UNCW (NA 96RU-0260), by the Biological Oceanography program at NSF (OCE-0550468) and NSF (OISE-0853089), and by the Spanish Government project CTM2007-66635.

References

1. Armstrong RA, Singh H, Torres J, Nemeth RS, Can A, Roman C, Eustice R, Riggs L, Garcia-Moliner G (2006) Characterizing the deep insular shelf coral reef habitat of the Hind Bank marine conservation district (US Virgin Islands) using the Seabed autonomous underwater vehicle. Continent Shelf Res 26:194–205

2. Bavestrello G, Cerrano C, Cattaneo-Vietti R, Calabria F, Cortesogno L, Sarà M (1996) Selective incorporation of foreign material in *Chondrosia reniformis*. Ital J Zool 63:215–220
3. Bayer K, Schmitt S, Hentschel U (2007) Microbial nitrification in Mediterranean sponges: possible involvement of ammonium-oxidizing *Betaproteobacteria*. In: Custódio M, Lôbo-Hajdu G, Hajdu E, Muricy G (eds) Porifera research: biodiversity, innovation, sustainability. Série Livros. Museu Nacional, Rio de Janeiro, pp 165–171
4. Bayer K, Schmitt S, Hentschel U (2008) Physiology, phylogeny and in situ evidence for bacterial and archaeal nitrifiers in the marine sponge *Aplysina aerophoba*. Environ Microbiol 10:2942–2955
5. Becerro MA (2008) Quantitative trends in sponge ecology research. Mar Ecol 29(2):167–177
6. Beman JM, Popp BN, Francis CA (2008) Molecular and biogeochemical evidence for ammonia oxidation by marine *Crenarchaeota* in the Gulf of California. ISME J 2:429–441
7. Buss LW, Jackson JBC (1979) Competitive networks: non-transitive competitive relationships in cryptic coral reef environments. Am Nat 113:223–234
8. Cerrano C, Calcinai B, Gioia Di Camillo C, Valisano L, Bavestrello G (2007) How and why do sponges incorporate foreign material? Strategies in Porifera. In: Custódio M, Lôbo-Hajdu G, Hajdu E, Muricy G (eds) Porifera research: biodiversity, innovation, sustainability. Série Livros. Museu Nacional, Rio de Janeiro, pp 239–246
9. Cowart JD, Henkel TP, McMurray SE, Pawlik JR (2006) Sponge orange band (SOB): a pathogenic-like condition of the giant barrel sponge, *Xestospongia muta*. Coral Reefs 25:513
10. Culman SW, Bukowski R, Gauch HG, Cadillo-Quiroz H, Buckley DH (2009) T-REX: software for the processing and analysis of T-RFLP data. BMC Bioinformatics 10:171
11. Diaz MC, Rutzler K (2001) Sponges: an essential component of Caribbean coral reefs. Bull Mar Sci 69:535–546
12. Diaz MC, Ward BB (1997) Sponge-mediated nitrification in tropical benthic communities. Mar Ecol Prog Ser 156:97–107
13. Diaz MC, Akob D, Cary CS (2004) Denaturing gradient gel electrophoresis of nitrifying microbes associated with tropical sponges. Boll Mus 1st Biol Univ Genova 68:279–289
14. Erguder TH, Boon N, Wittebolle L, Marzorati M, Verstraete W (2009) Environmental factors shaping the ecological niches of ammonia-oxidizing archaea. FEMS Microbiol Rev 33:855–869
15. Erwin PM, Thacker RW (2007) Incidence and identity of photosynthetic symbionts in Caribbean coral reef sponge assemblages. J Mar Biol Ass UK 87:1683–1692
16. Erwin PM, Thacker RW (2008) Cryptic diversity of the symbiotic cyanobacterium *Synechococcus spongiarum* among sponge hosts. Mol Ecol 17:2937–2947
17. Erwin PM, Thacker RW (2008) Phototrophic nutrition and symbiont diversity of two Caribbean sponge-cyanobacterial symbioses. Mar Ecol Prog Ser 362:139–147
18. Felsenstein J (1985) Confidence limits on phylogenies: an approach using the bootstrap. Evolution 39:783–791
19. Francis CA, Roberts KJ, Beman JM, Santoro AE, Oakley BB (2005) Ubiquity and diversity of ammonia-oxidizing archaea in water columns and sediments if the ocean. Proc Natl Acad Sci U S A 102:14683–14688
20. Fromont J, Garson M (1999) Sponge bleaching on the West and East coasts of Australia. Coral Reefs 18:340
21. Gammill ER, Fenner D (2005) Disease threatens Caribbean sponges: report and identification guide [WWW document]. URL http://www.reefbase.org/spongedisease
22. Gili J-M, Coma R (1998) Benthic suspension feeders: their paramount role in littoral marine food webs. TREE 13:316–321
23. Gómez R, Erpenbeck D, Van Dijk T, Richelle-Maurer E, Devijver C, Braekman JC, Woldringh C, van Soest RWM (2002) Identity of cyanobacterial symbionts of *Xestospongia muta*. Boll Mus Ist Biol Univ Genova 66–67:82–83
24. Hall TA (1999) BioEdit: a user-friendly biological sequence alignment editor and analysis program for Windows 95/98/NT. Nucleic Acids Symp 41:95–98
25. Hallam SJ, Konstantinidis KT, Putnam N, Schleper C, Watanabe Y, Sugahara J et al (2006) Genomic analysis of the uncultivated marine *crenarchaeote Cenarchaeum symbiosum*. Proc Natl Acad Sci USA 103:18296–18301
26. Hentschel U, Hopke J, Horn M, Friedrich AB, Wagner M, Hacker J, Moore BS (2002) Molecular evidence for a uniform microbial community in sponges from different oceans. Appl Environ Microbiol 68:4431–4440
27. Hentschel U, Usher KM, Taylor MW (2006) Marine sponges as microbial fermenters. FEMS Microbiol Ecol 55:167–177
28. Hoffmann F, Radax R, Woebken D, Holtappels M, Lavik G, Rapp HT et al (2009) Complex nitrogen cycling in the sponge *Geodia barretti*. Environ Microbiol. doi:10.1111/j.1462-2920.2009.01944.x
29. Holmes B, Blanch H (2007) Genus-specific associations of marine sponges with group I crenarchaeotes. Mar Biol 150:759–772
30. Jimenez E, Ribes M (2007) Sponges as a source of dissolved inorganic nitrogen: nitrification mediated by temperate sponges. Limnol Oceanogr 52:948–958
31. Jobb G (2008) TREEFINDER version of October 2008. Munich, Germany. Distributed by the author at www.treefinder.de
32. Kimes NE, Van Nostrand JD, Weil E, Zhou J, Morris PJ (2010) Microbial functional structure of *Montastraea faveolata*, an important Caribbean reef-building coral, differs between healthy and yellow-band diseased colonies. Environ Microbiol 12(2):541–556
33. Lam P, Jensen MM, Lavik G, McGinnis DF, Müller B, Schubert CJ et al (2007) Linking crenarchaeal and bacterial nitrification to anammox in the Black Sea. Proc Natl Acad Sci USA 104:7104–7109
34. Lee EY, Lee HK, Lee YK, Sim CJ, Lee JH (2003) Diversity of symbiotic archaeal communities in marine sponges from Korea. Biomol Eng 3:1–8
35. López-Legentil S, Song B, McMurray SE, Pawlik JR (2008) Bleaching and stress in coral reef ecosystems: *Hsp70* expression by the giant barrel sponge *Xestospongia muta*. Mol Ecol 17:1840–1850
36. Margot H, Acebal C, Toril E, Amils R, Puentes JLF (2002) Consistent association of crenarchaeal *Archaea* with sponges of the genus *Axinella*. Mar Biol 140:739–745
37. McMurray SE, Blum JE, Pawlik JR (2008) Redwood of the reef: growth and age of the giant barrel sponge *Xestospongia muta* in the Florida Keys. Mar Biol 155:159–171
38. McMurray SE, Henkel TP, Pawlik JR (2010) Demographics of increasing populations of the giant barrel sponge *Xestospongia muta* in the Florida Keys. Ecology 91:560–570
39. Meyer B, Kuever J (2008) Phylogenetic and spatial distribution of the microbial community associated with the Caribbean deep-water sponge *Polymastia* cf. *corticata* by 16S rRNA, *aprA*, and *amoA* gene analysis. Microb Ecol 56:306–321
40. Mohamed NM, Colman AS, Tal Y, Hill RT (2008) Diversity and expression of nitrogen fixation genes in bacterial symbionts of marine sponges. Environ Microbiol 10:2910–2921
41. Mohamed NM, Saito K, Tal Y, Hill RT (2009) Diversity of aerobic and anaerobic ammonia-oxidizing bacteria in marine sponges. ISME J. doi:10.1038/ismej.2009.84
42. Nagelkerken I, Aerts L, Pors L (2000) Barrel sponge bows out. Reef Encounter 28:14–15
43. Olson JB, Gochfeld DJ, Slattery M (2006) *Aplysina* red band syndrome: a new threat to Caribbean sponges. Mar Ecol Progr Ser 71:163–168
44. Osborne CA, Rees GN, Bernstein Y, Janssen PH (2006) New threshold and confidence estimates for terminal restriction

fragment length polymorphism analysis of complex bacterial communities. Appl Environ Microbiol 72:1270–1278
45. Øvreås L, Forney L, Daae FL, Torsvik V (1997) Distribution of bacterioplankton in meromictic lake Sælenvannet, as determined by denaturing gradient gel electrophoresis of PCR-amplified gene fragments coding for 16S rRNA. Appl Environ Microbiol 63:3367–3373
46. Pape T, Hoffmann F, Quéric N-V, von Juterzenka K, Reitner J, Michaelis W (2006) Dense populations of Archaea associated with demosponge *Tentorium semisuberites* Schmidt, 1870 from Arctic deep-waters. Polar Biol 29:662–667
47. Paul VJ, Ritson-Williams R (2008) Marine chemical ecology. Nat Prod Rep 25:662–695
48. Posada D, Crandall KA (1998) MODELTEST: testing the model of DNA substitution. Bioinformatics 14:817–818
49. Preston CM, Wu KY, Molinski TF, DeLong EF (1996) A psychrophilic crenarcheon inhabits a marine sponge: *Cenarchaeum symbiosum* gen. nov., sp. nov. Proc Natl Acad Sci USA 93:6241–6246
50. Rotthauwe J-H, Witzel K-P, Liesack W (1997) The ammonia monooxygenase structural gene *amoA* as a functional marker: molecular fine-scale analysis of natural ammonia-oxidizing populations. Appl Environ Microbiol 63:4704–4712
51. Schleper C, Jurgens G, Jonuscheit M (2005) Genomic studies of uncultivated *Archaea*. Nat Rev Microbiol 3:479–488
52. Southwell MW, Weisz JB, Martens CS, Lindquist N (2008) In situ fluxes of dissolved inorganic nitrogen from the sponge community on Conch Reef, Key Largo, Florida. Limnol Oceanogr 53:986–996
53. Stahl DA, Amann R (1991) Development and application of nucleic acid probes in bacterial systematics. In: Stackebrandt E, Goodfellow M (eds) Nucleic acid techniques in bacterial systematics. Wiley, Chichester, pp 205–248
54. Steindler L, Hucheon D, Avni A, Ilan M (2005) 16S rRNA phylogeny of sponge associated cyanobacteria. Appl Environ Microbiol 71:4127–4131
55. Steger D, Ettinger-Epstein P, Whalan S, Hentschel U, de Nys R, Wagner M, Taylor MW (2008) Diversity and mode of transmission of ammonia-oxidizing archaea in marine sponges. Environ Microbiol 10:1087–1094
56. Tamura K, Dudley J, Nei M, Kumar S (2007) MEGA 4: Molecular Evolutionary Genetic Analysis (MEGA) software version 4.0. Mol Biol Evol 24:1596–1599
57. Tavaré S (1986) Some probabilistic and statistical problems in the analysis of DNA sequences. In: Miura RM (ed) Some mathematical questions in biology—DNA sequence analysis. Am Math Soc, Providence, RI, pp 57–86
58. Taylor MW, Radax R, Steger D, Wagner M (2007) Sponge-associated microorganisms: evolution, ecology, and biotechnological potential. Microbiol Mol Biol Rev 71(2):295–347
59. Taylor MW, Hill RT, Piel J, Thacker RW, Hentschel U (2007) Soaking it up: the complex lives of marine sponges and their microbial associates. ISME J 1:187–190
60. Teragawa CK (1986) Particle transport and incorporation during skeleton formation in a keratose sponge *Dysidea etheria*. Biol Bull 170:321–334
61. Thacker R (2005) Impacts of shading on sponge-cyanobacteria symbioses: a comparison between host-specific and generalist associations. Integr Comp Biol 45:369–376
62. Thompson JD, Gibson TJ, Plewniak F, Jeanmougin F, Higgins DG (1997) The CLUSTAL_X windows interface: flexible strategies for multiple sequence alignment aided by quality analysis tools. Nucleic Acids Res 25:4876–4882
63. Usher KM, Fromont J, Sutton DC, Toze S (2004) The biogeography and phylogeny of unicellular cyanobacterial symbionts in sponges from Australia and the Mediterranean. Microb Ecol 48:167–177
64. Venter JC, Remington K, Heidelberg JF, Halpern AL, Rusch D, Eisen JA et al (2004) Environmental genome shotgun sequencing of the Sargasso Sea. Science 304:5667
65. Vicente VP (1990) Response of sponges with autotrophic endosymbionts during the coral-bleaching episode in Puerto Rico (West Indies). Coral Reefs 8:199–202
66. Waksman SA, Hotchkiss M, Carey CL (1933) Marine bacteria and their role in the cycle of life in the sea. Biol Bull LXV:137–167
67. Webster N (2007) Sponge disease: a global threat? Environ Microbiol 9:1363–1375
68. Webster N, Watts JEM, Hill RT (2001) Detection and phylogenetic analysis of novel Chrenarchaeote and Euryarchaeote 16S ribosomal rRNA gene sequences from a Great Barrier Reef sponge. Mar Biotechnol 3:600–608
69. Webster N, Negri AP, Munro MMHG, Battershill CN (2004) Diverse microbial communities inhabit Antarctic sponges. Environ Microbiol 6:288–300
70. Wuchter C, Abbas B, Coolen MJL, Herfort L, van Bleijswijk J, Timmers P et al (2006) Archaeal nitrification in the ocean. Proc Natl Acad Sci USA 103:12317–12322
71. Zea S (1993) Cover of sponges and other sessile organisms in rocky and coral reef habitats of Santa Marta, Colombian Caribbean Sea. Caribb J Sci 29:75–88